Soft Pneumatic Pads Enable New Sensing and Actuation Capabilities in Soft-Rigid Grippers

Soft pneumatic pads enable new sensing and actuation capabilities in soft-rigid grippers

Maria Pozzi[1,2], Leonardo Franco[1], Zubair Iqbal[1],
Monica Malvezzi[1], Domenico Prattichizzo[1,2], and Gionata Salvietti[1]

***Abstract*— Contact force sensing and grasp adaptation in soft robotic hands are still open challenges, although they represent fundamental requirements towards the achievement of delicate and accurate in-hand manipulation. In this paper, we present soft pneumatic pads that can be embedded into the rigid phalanges of a soft-rigid gripper to sense contact forces and consequently adapt the contact locations and grasping forces. Each pad is connected to a pressure sensor and can be independently inflated/deflated. The pads add sensing and actuation capabilities to the gripper. As a proof of concept, we present three applications where they are used for contact detection, in-hand manipulation, and grasp adjustment.**

I. Introduction

Grasping and manipulation are contact-rich tasks requiring robots to touch the object and possibly the environment in multiple different locations. Current robotic hands, however, rarely embed enough sensors to reconstruct on-line the whole dynamics of hand-object and hand-environment interactions. This is especially true for underactuated and compliant hands, whose features lead to "different requirements and opportunities for perception" [1]. On the one hand, differently from rigid devices, since a single actuator typically controls several degrees of freedom, it is difficult to rely only on the sensors embedded in the actuators to reconstruct the gripper configuration. On the other hand, the use of highly deformable materials enables new sensing solutions exploiting softness [2], [3], [4].

This paper introduces a new soft-rigid phalanx that embeds a *soft pad*, i.e., a small pneumatic chamber that can be used for pressure sensing and as an additional actuator through inflation/deflation. In principle, the proposed solution could be adapted to any type of robotic gripper, but here we focus on tendon-driven ones, presenting the fabrication and use of the *SoftPad Gripper* (Fig. 1). The proposed gripper embeds a soft pad in each of its rigid phalanges. By evaluating the pressure variations inside each pad, it is possible to detect which phalanges are in contact with the grasped object. A similar principle was adopted in [5] to sense objects over a matrix of pneumatic actuators.

[1]Department of Information Engineering and Mathematics, University of Siena, Siena, Italy ({name.surname}@unisi.it).

[2]Humanoids & Human Centered Mechatronics Research Line, Istituto Italiano di Tecnologia, Genoa, Italy

*We acknowledge the support of the European Union by the Next Generation EU project ECS00000017 "Ecosistema dell'Innovazione" Tuscany Health Ecosystem (THE, PNRR: Spoke 9 - Robotics and Automation for Health), and by the Horizon Europe project "HARIA - Human-Robot Sensorimotor Augmentation - Wearable Sensorimotor Interfaces and Supernumerary Robotic Limbs for Humans with Upper-limb Disabilities" (GA No. 101070292).

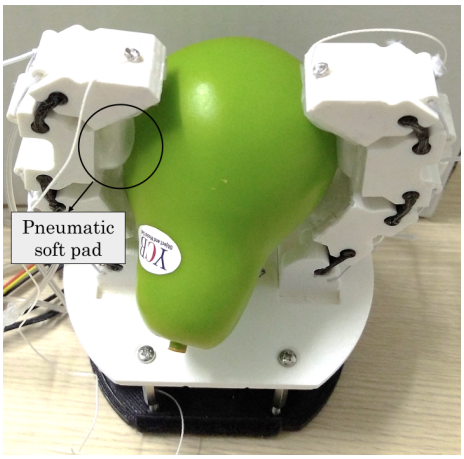

Fig. 1: Grasp performed by the SoftPad Gripper, a tendon-driven gripper equipped with pneumatic pressure sensors.

Pneumatic devices can be used for sensing purposes, but can also be actuated by inflating/deflating them. By changing the internal pressure of the pads it is possible to vary the sensing capabilities of the device (e.g., sensitive area, sensitivity, measurement range), and stiffness properties [5]. In addition, when applied to a gripper, each pad adds an extra possible motion to the phalanx which can be expanded or compressed by changing the inflating pressure. This can be useful to vary the force exerted at a certain phalanx, to add or remove contact points from a grasp, and to move the object in-hand.

In this work, first a characterization of the sensing capabilities of the pads is conducted. Then, proof-of-concept experiments show how the new sensing and actuation capabilities and their interplay can be exploited in grasping and in-hand manipulation tasks.

II. Related Works: Sensors for Soft Hands

Soft and compliant grippers have two main issues to be solved in terms of sensing. The first is related to the proprioception of the hand posture. Differently from rigid hands where encoders and other sensors can be used to measure joint variables, in soft structures determining the actual position of the fingers is one of the main challenges. Several solutions have been proposed, ranging from optic fiber [6] to strain sensors [7]. Moreover, sensors designed for soft robotic systems need to be stretchable, flexible, and reliable to measure deformation modes like contraction,

extension, twisting, and bending [8], [9]. An overview of sensing techniques for soft robots can be found in [10].

The other important issue related to sensing in soft hands is that of determining contact forces. In this paper, we tackle this problem focusing in particular on tendon-driven grippers in which the flexion/extension motions can be controlled by measuring the length of the tendons, but still the final position of the contact points on the objects is difficult to determine as it is the result of complex hand-object interactions depending also on the compliance of the joints.

Different sensors that can be used in manipulation tasks have been proposed in literature [11], [12], [13]. When it comes to soft hands, adopted technologies include piezoelectric polymer contact sensors [14], force sensitive resistors (FSRs) [15], and also solutions which inherently exploit the hand softness. In [16], for example, a novel tactile sensor based on magnetic sensing and soft materials is presented. Another interesting approach considers the use of acoustic sensors inside soft pneumatic actuators. By measuring how the sound is modulated through the soft structure, it is possible to recognize sound changes and compute the corresponding contact locations [17].

In this work, we adopt pneumatic sensing for detecting contact points based on the variation of internal pressure inside a suitably designed soft structure. This principle has been adopted in previous works not only to design sensors for robotic fingers and hands [18], [19], [20], [21], but also in exoskeletons [18], and in teleoperation setups [22]. The main advantage of pneumatic sensors is that the related electronics can be placed far from the sensitive area, allowing to build systems which can be easily washed or used in environments where bringing electronic components might be unsafe (e.g., underwater). While most of previous works focus on building purely sensing devices, the proposed pad can be inflated/deflated to obtain extra degrees of actuation. This is not feasible, for example, in soft pneumatic mechanosensors which contain multiple cavities embedded into a larger deformable structure [23], [24].

III. Device Design

A. Soft Pad

The proposed soft pad is a pneumatic chamber having a length and width of 18×16 mm, respectively. The total height is 8 mm, with an inflation layer with thickness 1.5 mm.

For developing the pads, we followed similar guidelines as those described in [25], [26]. The used material is the EcoFlex™ silicone (Smooth-On Inc., USA) with shore hardness of 00-30 [27]. It is a versatile and easy to use platinum-catalyzed silicone that comes with two parts: A and B. The optimal mixing ratio (weight or volume) to achieve a smooth and well cured elastomer is $A/B = 1$. The CAD model and the prototype of a single phalanx embedding a soft pad are shown in Fig. 2.

The fabrication of a soft pad consists of three steps. Initially, a base for the inflation layer is created by pouring a 1:1 mixture of A and B silicone in the rigid phalanx that has a cavity with a suspended grid which serves as an anchoring structure once the silicone is cured (Fig. 2b). The silicone takes 4-5 hrs to cure properly. The second step is to place over the base an Acetate sheet or mold release of the size of the inflation layer. In the proposed device, the inflation layer is $13 \times 11 \times 1.5$ mm. The final step is to pour again the mixture of A and B silicone, and let it cure for 4-5 hrs.

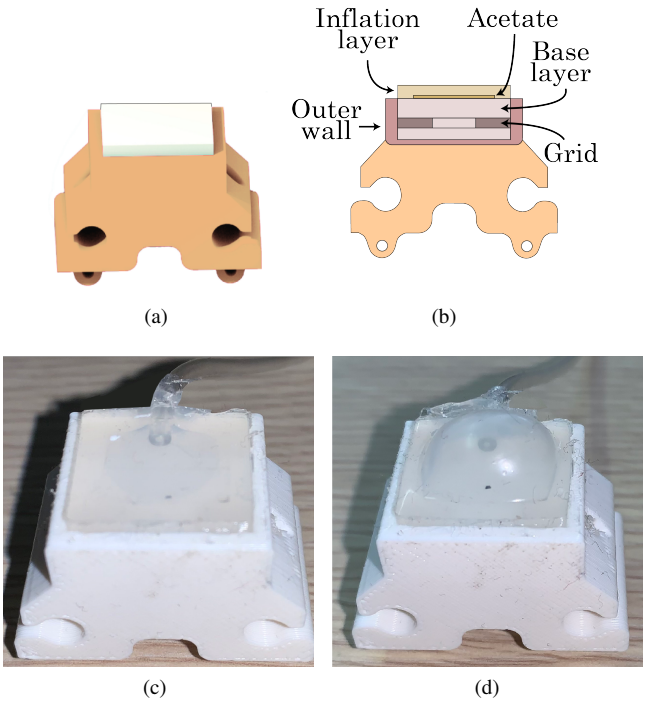

Fig. 2: (a) CAD model of the phalanx, (b) cross section view showing how the soft pad is embedded inside the rigid phalanx, (c) phalanx prototype with deflated soft pad, (d) phalanx prototype with inflated soft pad.

All the soft pads are connected to a compact control system, called Pneumaticbox [28], that is used to control their inflation and deflation. The Pneumaticbox was developed to enable an efficient control of soft actuators and it can provide up to eight independently controlled channels, each equipped with two discrete valves for inflation and deflation, and a differential pressure sensor. All sensors and valves are connected to a BeagleBone®Black (BeagleBoard.org, USA) embedded computer which is the main processing unit for the Pneumaticbox.

B. SoftPad Gripper

By assembling six phalanges equipped with a soft pad each, a two-fingered gripper with three phalanges per finger was built, obtaining a modular structure similar to that adopted in previous works [29], [30]. The developed prototype of the SoftPad Gripper is shown in Fig. 3, whereas its technical features are listed in Table I.

The proposed gripper has a soft-rigid structure in which rigid phalanges are connected by flexible joints. The rigid parts are made of ABS (Acrylonitrile Butadiene Styrene, ABSPlus, Stratasys, USA) using Fused Deposition Modelling

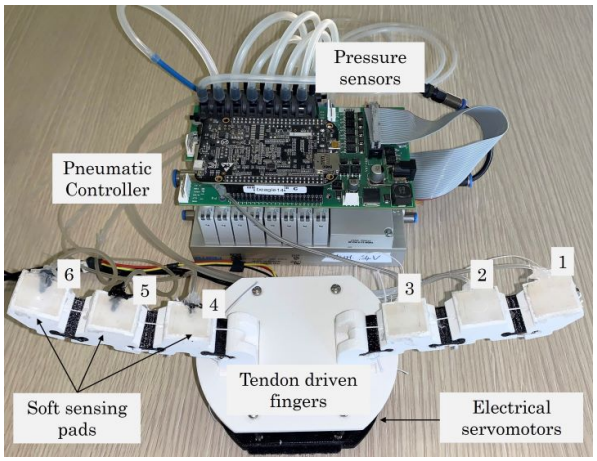

Fig. 3: The SoftPad Gripper and its pneumatic controller. The numeration of the phalanges corresponds to that adopted in the experiments.

TABLE I: Technical features of the SoftPad Gripper.

Technical Features	
Weight (including motors)	480 g
Max. actuator torque	3.1 Nm @ 12 V
Max. current	2.8 A @ 12 V
Continuous operating time	3.5 h @stall torque
Max. operating angles	300 deg, endless turn
Max. non-loaded velocity	684 deg/s

Material and Size Parameters	**Flexible Part (Joint)**	**Stiff Part (Phalanx)**
Material type	TPU	ABS
Modulus of elasticity (E)	15.2 MPa	40 MPa
Shore Hardness	$85A$	$70D$
Density	1200 kg/m^3	1070 kg/m^3
width	20 mm	20 mm
length	14 mm	33 mm
height	2.1 mm	21 mm

(FDM), whereas the flexible parts are made of Thermoplastic Polyurethene (TPU). Thanks to its high elongation, the TPU material allows for repeated movement and impact without wear or cracking, proving also an excellent vibration reduction. The assembly of the finger is done by sliding the flexible parts inside the rigid parts, without the need of any other fixation step.

Each finger is actuated by a Dynamixel Servo Motor MX-28AT. Both fingers are actuated using a tendon driven approach, each rigid phalanx contains a hole which serves as a passage for the tendon. The Arbotix-M controller (Robotis, South Korea) is used to control the two actuators. The complete system is shown in Fig. 3.

IV. Characterization of the Soft Pads

Two experiments were conducted to characterize the functioning of the soft pads. Experiment 1 aimed at analysing how the size of the inflated part of the pad varies with the internal pressure when no load is applied to the external pad surface. Experiment 2 was conducted to characterize the relation between sensed internal pressure and applied force.

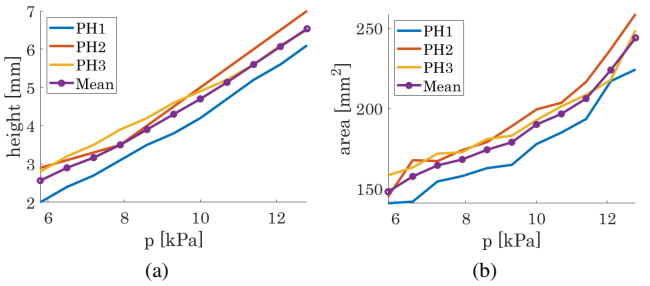

Fig. 4: Soft pads of the first finger: size ((a) height, (b) area) of the inflated part with respect to the internal pressure. Variations among the pads in the three phalanges (PH1, PH2, PH3) are due to uncertainties in the fabrication process.

A. Experiment 1: height and sensitive area of the sensor

To characterize the presented sensing pad, we analysed how the height, length, and width of the inflated part of the pad vary with respect to the internal pressure. Measurements were performed using a high-precision calibre (0.01 mm resolution). Obtained results in terms of height for the phalanges of the first finger are shown in Fig. 4a. The reported measurements are the maximum values reached by the inflated part of the pad. The length and the width followed a similar trend as the height, but we did not report them for the sake of brevity. Instead, we chose to show the area of the rectangle at the base of the inflated volume pad, computed by multiplying the length and the width at each pressure value (Fig. 4b). As expected, all studied quantities tend to increase when the inflating pressure increases. Differences among phalanges are due to uncertainties on the pad size introduced in the fabrication process. However, the deviation from the average behaviour is in the order of tenth of millimetres (e.g., the maximum root mean square error between a phalanx and the average behaviour is the one computed for the height of phalanx 1: $RMSE_{H1} = 0.4634$ mm).

B. Experiment 2: force sensing

To characterize the relationship between the sensed internal pressure of the pad and the force applied to it, we built an experimental setup in which an ATI Nano17 six-axis force/torque sensor (ATI Industrial Automation, USA) is pressed against an inflated pad using a linear actuation system (Fig. 5a). The latter is obtained by attaching a Dynamixel Servo Motor to a rack and pinion mechanism which transforms the rotational motion of the motor shaft into a translational motion of the 3D-printed link embedding the F/T sensor. To convert the encoder tick value to the translation in millimetres we used the following equation

$$\Delta z_{mm} = \Delta z_{tick} \cdot c_f \cdot \frac{\pi}{180} \cdot r_{pitch},$$

where c_f is the tick-degrees conversion factor and r_{pitch} is the pitch radius of the gear in millimetres.

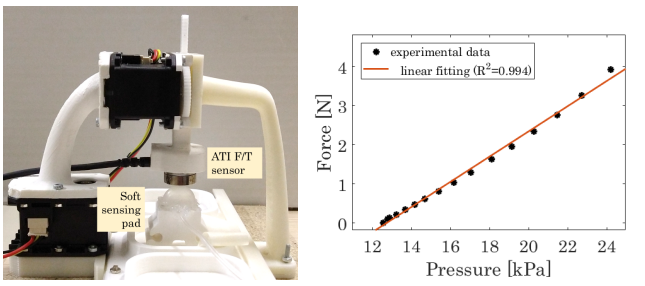

(a) (b)

Fig. 5: (a) Experimental setup to characterize the soft pads in terms of pressure/force relationship. (b) Average values of pressure and force obtained for 16 probe positions (15 positions plus the initial position where there is no contact), and corresponding linear fitting.

We developed an application in LabVIEW 2019 to both control the servomotor and read the z-axis force (normal to the pad surface) sensed by the ATI force sensor in real-time. At the beginning of each data acquisition, we inflated the pad to a fixed and stable pressure p_i. We positioned the force sensor in contact with the inflated pad, saving the starting position of the linear actuator, determining $z_{contact}$. Then we proceeded to lower the position of the actuator until the force sensor came in contact with the bottom of the pad, determining z_{max}. We then obtained Δz_i, the working range of the pad at a certain inflation pressure p_i, as $\Delta z_i = |z_{max} - z_{contact}|$. This range was then quantized in 15 measuring steps. During the acquisition we saved the time, the position of the linear actuator by reading the 12 bit absolute encoder of the servomotor, and the z component of the ATI force sensor. An example of force and position acquired data for an initial internal pressure of 12.6 kPa is shown in Fig. 6.

In Fig. 7, the sensed force versus the probe position is reported for different initial inflation pressures. It can be noticed that there is a quadratic relationship between force and position. In addition, the more the pad is inflated, the larger is the displacement that can be applied to it without seeing it collapsing, and thus the larger is the set of applied forces that can be sensed. This is why when $p_i = 12.6$ kPa (violet plot) there are data points also in the top-right part of the graph, whereas in the other cases there are less points.

With the same procedure as that described above, we recorded the pressure-force relation when the pad was initially inflated at 12.6 kPa. We used the same probe position range as that employed in the previous experiments and for each of the 15 positions we recorded the force along the z-axis of the ATI sensor and the internal pressure sensed by the pressure sensor connected to the pad. This process was repeated 3 times, obtaining 3 pressure and 3 force values for each probe position. Obtained results were averaged and reported in Fig. 5b. The higher is the applied force, the more the internal pressure of the pad increases, and this growth is almost linear.

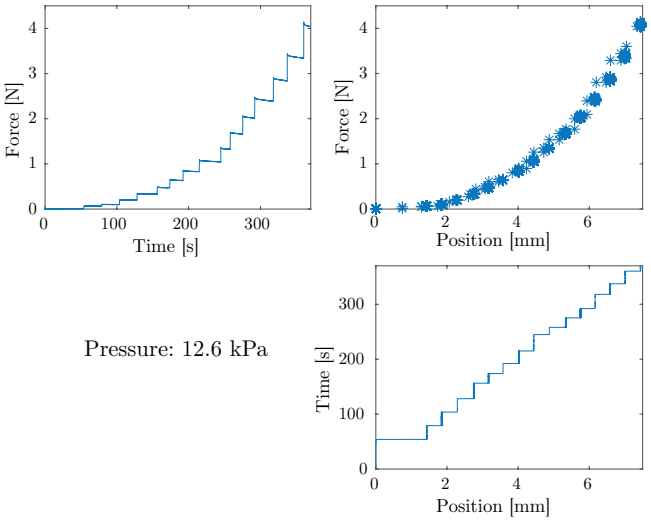

Fig. 6: Data collected during the soft pads characterization. (Top-left) sensed force with respect to time, (Bottom-right) position of the probe with respect to time, and (Top-right) force with respect to position.

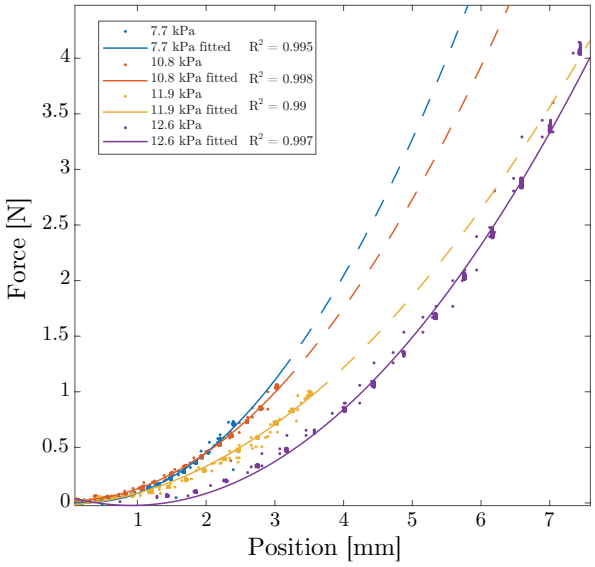

Fig. 7: Data fitting of the force-position characteristic curve. Notably, all distributions fitted as quadratic polynomials.

V. Experiments with the SoftPad Gripper

To show how the soft pads can be used in grasping and manipulation tasks, the SoftPad Gripper was tested in three different tasks which serve as proof-of-concept demonstrations of the dual function (sensing, actuation) of the pads.

A. Contact detection

To demonstrate the usefulness of the pads from the sensing point of view, they have been applied in a contact detection task. As shown in Fig. 8, six different objects were grasped with the gripper and the initial and final pressures read by the pads were recorded. Table II shows the obtained values. Those corresponding to the contacting pads are written in

Fig. 8: SoftPad Gripper grasping six different objects.

TABLE II: Sensed internal pressure inside the soft pads before and after the grasp for each object. Values in bold indicate the final pressure of phalanges that are detected as in contact with the object.

Objects	Pressure in the Phalanges (kPa)					
	PH1	**PH2**	**PH3**	**PH4**	**PH5**	**PH6**
Apple	12.44	12.43	12.56	12.63	12.50	12.48
	12.81	**16.87**	**19.02**	**20.84**	**13.33**	12.44
Lemon	12.08	12.38	12.36	12.28	12.44	12.49
	11.81	12.32	**15.39**	**15.18**	12.32	12.47
Pear	11.58	12.28	12.24	12.07	12.29	12.46
	11.31	**16.20**	**16.90**	**18.69**	**13.73**	12.44
Ball	12.42	12.47	12.68	12.58	12.78	12.49
	14.08	**16.10**	**17.87**	**16.71**	**16.05**	**14.25**
Cylinder	12.19	12.39	12.59	12.39	12.72	12.54
	14.32	**16.15**	**19.66**	**21.32**	**14.14**	**13.22**
Box	11.99	12.35	12.56	12.26	12.66	12.54
	16.49	**17.49**	**12.73**	**22.74**	**17.58**	**12.74**

bold. A contact is detected when the variation between the initial pressure and the final pressure after the grasp goes above a certain threshold ($t_c = 0.05$ kPa in our experiments). To show the versatility of the gripper we chose objects with different shapes and material properties. The plastic apple (mass $m = 68$ g, diameter $d = 75$ mm), the yellow container ($m = 38$ g, 100×78 mm), and the box ($m = 187$ g, $35 \times 110 \times 89$ mm) have prototypical shapes: sphere, cylinder, and cuboid, respectively. The other objects were chosen as representatives of objects with irregular shapes (pear, $m = 49$ g, 66.2×100 mm), soft objects (basket ball, $m = 20$ g, $d = 100$ mm), and small objects with respect to the fingers (lemon, $m = 29$ g, 24×68). All objects except for the ball belong to the YCB Dataset [31]. The conducted tests show that the proposed gripper is versatile enough to grasp different objects, and that the sensing pads can effectively be used to detect the contacting phalanges.

TABLE III: Cylinder displacement in the horizontal and in the vertical directions and for the two configurations.

Object	**Dir.**	**Disp. [mm]** (mean±std)	**Disp. [mm]** (total)
Config. 1	H	3.30 ± 0.28	3.58
	V	0.16 ± 0.18	0.61
Config. 2	H	2.95 ± 0.23	2.99
	V	-0.86 ± 0.2	0.05

B. In-hand manipulation

The pneumatic pads can also be used to augment the otherwise limited in-hand manipulation capabilities of underactuated soft-rigid grippers. To show an example of this application, we chose to implement the horizontal translation of the object with respect to the palm. The tendons were kept at the same length during the task, whereas the internal pressure of the pads was regulated to obtain a translation from left (phalanges PH2, PH3 inflated) to right (phalanges PH4, PH5 inflated), and viceversa. We tested this task with a cylindrical object (14 g, 60×62 mm) from the YCB dataset. The object was placed in two different configurations (Config. 1: vertical, Config. 2: horizontal), as shown in Fig. 9. We selected a rigid object so that the pad inflation would result in a motion and not in a deformation. The cylinder size was chosen to fit within the fingers, so that the object was in contact with all the selected phalanges.

In each cylinder configuration, the fingers were closed over the object so that all the involved phalanges were in contact. Then, five experimental trials were performed. In each trial, the object is moved from left to right and back. The object displacement in the gripper plane was measured by processing the videos of the experiments through the Tracker Software [32]. Ideally, we expected a relevant and repeatable horizontal (H) displacement, and a small vertical (V) displacement. In Table III, the mean and the standard deviation of the displacement and its total value, computed from the initial position to the final position after five trials, are reported.

The gathered data show that, on average, the horizontal in-hand translation was successfully carried out with a relatively low displacement in the vertical direction. When the cylinder was held in the vertical position, the average vertical displacement of the object was lower. We observed that, in Config. 1, the obtained vertical translation in the single trials is low (low mean value), but after five trials the object is displaced of more than half millimeter in total. In Config. 2, the object is mainly displaced along the horizontal direction, however, every time the object is shifted towards finger 1 (right), it is also pushed a bit downwards. This is due to the pushing action of the pad in PH5 (see Fig. 9, bottom-right). When the object is pushed back to the left, it goes up again. As a result, in Config. 2, after each trial the object goes back to the same position, leading to a negligible total vertical displacement.

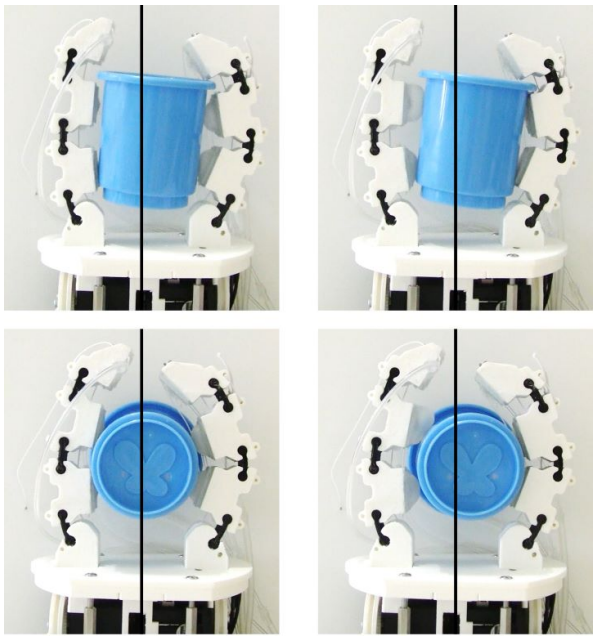

Fig. 9: In-hand horizontal translation (from left to right) of a cylinder in two configurations (top row: Config. 1, bottom row: Config. 2). The black line serves as a reference to clearly perceive the object motion.

C. Grasp adjustment

To show an example of how the added sensing and actuation capabilities can be used together, we implemented a grasp adjustment task in which the internal pressures of the pads were iteratively regulated to get a similar pressure at all the contacts. In particular, once the pads in contact with the grasped object were detected, the smallest value of internal pressure was chosen and used as goal pressure for the other contacting pads. The latter were then inflated/deflated to get an internal pressure in a certain range with respect to the target value (in our case: $p_{goal} \pm 2$ kPa). Fig. 10 shows results obtained for a power grasp of a cylinder ($m = 19$ g, 70×35 mm). We plotted only the final stable pressures reached at the end of each phase of the task (i.e, grasp achievement and ends of adjustment steps), neglecting transitory phases for the purpose of visualization. As shown in Fig. 10, the contacting phalanges are PH2, PH3, PH4, and PH5. The one having the lowest internal pressure after the contact is PH4 ($p_{goal} = 13.13$ kPa). Thus, pads 2, 3, and 5 are deflated for an amount of time depending on the difference between the current and goal pressures. At the successive step, the PH2 is deflated again while PH3 is inflated as it reached a too low pressure value. PH5 is deflated by the algorithm, but this does not have a clear effect, as its pressure increases due to the fact that the inflated PH3 presses on the object and thus also on PH4 and PH5. At the second last step, PH2 is inflated, while PH3 and PH5 are deflated. At the last step, PH3 is deflated and the other pressures vary due to this deflation. Lastly, the algorithm stops as the final pressure values are within the selected range

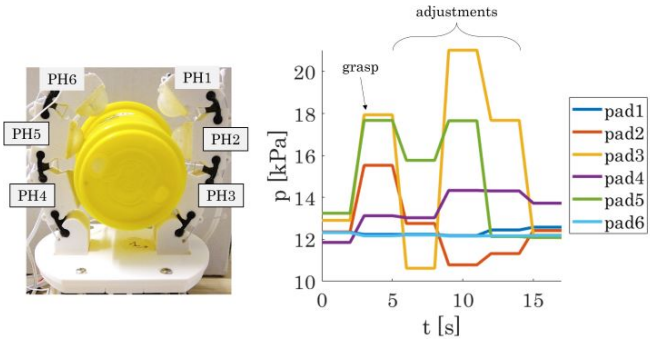

Fig. 10: Pressure re-distribution in the grasp of a cylinder.

with respect to the goal: $p_2 = 12.42$ kPa, $p_3 = 12.21$ kPa, $p_4 = 13.75$ kPa, $p_5 = 12.09$ kPa.

VI. Conclusions

This paper introduces a new soft-rigid tendon-driven gripper with pneumatically actuated soft pads embedded in its phalanges. We characterized the soft pads in terms of sensed pressure and force ranges, and we showed that the pads can be used as sensing and actuation devices in different tasks: contact detection, in-hand manipulation, and contact pressure distribution adjustment.

The proposed gripper has advantages and disadvantages. The first advantage is clearly represented by the fact that the SoftPad Gripper combines the shape adaptability of soft hands with the possibility of monitoring contact forces. This could be particularly useful when handling delicate objects. Indeed, their possible damage could be prevented by redistributing contact pressures among the detected contact points, avoiding localized peak forces.

Thanks to the gripper features, if very tight grasps are needed, e.g. to manipulate rigid and heavy objects, the pads can be deflated and the gripper acts as a classic soft-rigid structure. When delicate grasps have to be performed, the soft pads can be inflated and used to gently interact with the object.

Another positive aspect of the SoftPad Gripper is represented by the absence of electronic components in the fingers and in the palm. This could allow, for instance, the finger to be washed or sterilized as it may be used to manipulate food or other fragile items.

Concerning the disadvantages, introducing pneumatic actuated pads sensibly increases the complexity of the system requiring a supplementary effort for its control. Moreover, pneumatic actuation comes with the need of an additional controller to regulate valves and with the need for pressurized air supply that may be easily available in an industrial setup, while it may require supplementary components in other contexts. Another limitation of the proposed device is that the fabrication process combining rigid links with soft pads needs a high accuracy to avoid possible leakages, especially at the connection between the pad and the pipes. We are currently evaluating the adoption of different fabrication techniques for the pads (e.g., 3-D printing [20]).

As preliminarily demonstrated in this paper, the soft pads could be exploited as an additional source of actuation for in-hand manipulation. It has been recently shown that softness can make in-hand manipulation more robust [33]. In future work, we will build upon this concept exploring how the combination of two kinds of actuation systems (tendon-driven and pneumatic) can be leveraged to regulate joint and contact compliance [34], and thus obtain desired dexterous motions.

REFERENCES

[1] A. Bicchi and O. Brock, "Editorial," *The International Journal of Robotics Research*, vol. 39, no. 14, pp. 1601–1603, 2020. [Online]. Available: https://doi.org/10.1177/0278364920962422

[2] M. Tavakoli, P. Lopes, J. Lourenço, R. P. Rocha, L. Giliberto, A. T. de Almeida, and C. Majidi, "Autonomous selection of closing posture of a robotic hand through embodied soft matter capacitive sensors," *IEEE Sensors Journal*, vol. 17, no. 17, pp. 5669–5677, 2017.

[3] Y. Yang and Y. Chen, "Innovative design of embedded pressure and position sensors for soft actuators," *IEEE Robotics and Automation Letters*, vol. 3, no. 2, pp. 656–663, 2018.

[4] M. Ntagios, H. Nassar, A. Pullanchiyodan, W. T. Navaraj, and R. Dahiya, "Robotic hands with intrinsic tactile sensing via 3d printed soft pressure sensors," *Advanced Intelligent Systems*, vol. 2, no. 6, p. 1900080, 2020.

[5] C. Gaudeni, M. Pozzi, Z. Iqbal, M. Malvezzi, and D. Prattichizzo, "Grasping with the softpad, a soft sensorized surface for exploiting environmental constraints with rigid grippers," *IEEE Robotics and Automation Letters*, vol. 5, no. 3, pp. 3884–3891, 2020.

[6] L. U. Odhner, L. P. Jentoft, M. R. Claffee, N. Corson, Y. Tenzer, R. R. Ma, M. Buehler, R. Kohout, R. D. Howe, and A. M. Dollar, "A compliant, underactuated hand for robust manipulation," *The International Journal of Robotics Research*, vol. 33, no. 5, pp. 736–752, 2014.

[7] M. Amjadi, K.-U. Kyung, I. Park, and M. Sitti, "Stretchable, skin-mountable, and wearable strain sensors and their potential applications: a review," *Advanced Functional Materials*, vol. 26, no. 11, pp. 1678–1698, 2016.

[8] C. Tawk and G. Alici, "A review of 3d-printable soft pneumatic actuators and sensors: Research challenges and opportunities," *Advanced Intelligent Systems*, vol. 3, no. 6, p. 2000223, 2021.

[9] J. Shintake, V. Cacucciolo, D. Floreano, and H. Shea, "Soft robotic grippers," *Advanced materials*, vol. 30, no. 29, p. 1707035, 2018.

[10] H. Wang, M. Totaro, and L. Beccai, "Toward perceptive soft robots: Progress and challenges," *Advanced Science*, vol. 5, no. 9, p. 1800541, 2018.

[11] R. D. Howe, "Tactile sensing and control of robotic manipulation," *Advanced Robotics*, vol. 8, no. 3, pp. 245–261, 1993.

[12] J. Tegin and J. Wikander, "Tactile sensing in intelligent robotic manipulation–a review," *Industrial Robot: An International Journal*, vol. 32, no. 1, pp. 64–70, 2005.

[13] H. Yousef, M. Boukallel, and K. Althoefer, "Tactile sensing for dexterous in-hand manipulation in robotics—a review," *Sensors and Actuators A: Physical*, vol. 167, no. 2, pp. 171 – 187, 2011, solid-State Sensors, Actuators and Microsystems Workshop. [Online]. Available: http://www.sciencedirect.com/science/article/pii/S0924424711001105

[14] A. M. Dollar, L. P. Jentoft, J. H. Gao, and R. D. Howe, "Contact sensing and grasping performance of compliant hands," *Autonomous Robots*, vol. 28, no. 1, pp. 65–75, 2010.

[15] F. Vigni, E. Knoop, D. Prattichizzo, and M. Malvezzi, "The role of closed-loop hand control in handshaking interactions," *IEEE Robotics and Automation Letters*, vol. 4, no. 2, pp. 878–885, April 2019.

[16] L. Jamone, L. Natale, G. Metta, and G. Sandini, "Highly sensitive soft tactile sensors for an anthropomorphic robotic hand," *IEEE sensors Journal*, vol. 15, no. 8, pp. 4226–4233, 2015.

[17] G. Zöller, V. Wall, and O. Brock, "Active acoustic contact sensing for soft pneumatic actuators," in *2020 IEEE International Conference on Robotics and Automation (ICRA)*. IEEE, 2020, pp. 7966–7972.

[18] N. Cheng, J. H. Low, B. W. Ang, A. J. Goh, and C.-H. Yeow, "Soft fabric-based pneumatic sensor for bending angles and contact force detection," *IEEE Sensors Journal*, vol. 19, no. 4, pp. 1269–1279, 2018.

[19] C. Tawk, H. Zhou, E. Sariyildiz, M. In Het Panhuis, G. M. Spinks, and G. Alici, "Design, modeling, and control of a 3d printed monolithic soft robotic finger with embedded pneumatic sensing chambers," *IEEE/ASME Transactions on Mechatronics*, vol. 26, no. 2, pp. 876–887, 2020.

[20] O. Shorthose, A. Albini, L. He, and P. Maiolino, "Design of a 3d-printed soft robotic hand with integrated distributed tactile sensing," *IEEE Robotics and Automation Letters*, vol. 7, no. 2, pp. 3945–3952, 2022.

[21] H. Zhou, C. Tawk, and G. Alici, "A 3d printed soft robotic hand with embedded soft sensors for direct transition between hand gestures and improved grasping quality and diversity," *IEEE Transactions on Neural Systems and Rehabilitation Engineering*, vol. 30, pp. 550–558, 2022.

[22] C. Gaudeni and D. Prattichizzo, "A mathematical model of the pneumatic force sensor for robot-assisted surgery," in *IEEE World Haptics Conference 2019*, Tokyo, Japan, July 2019, pp. 598–603.

[23] S. E. Navarro, O. Goury, G. Zheng, T. M. Bieze, and C. Duriez, "Modeling novel soft mechanosensors based on air-flow measurements," *IEEE Robotics and Automation Letters*, vol. 4, no. 4, pp. 4338–4345, 2019.

[24] H. Choi and K. Kong, "A soft three-axis force sensor based on radially symmetric pneumatic chambers," *IEEE Sensors Journal*, vol. 19, no. 13, pp. 5229–5238, 2019.

[25] Soft Robotics Toolkit. (2016) Soft gripper fabrication guide. Accessed: 2024-02-29. [Online]. Available: https://biodesign.seas.harvard.edu/soft-robotics-toolkit-0

[26] V. Ruiz Garate, M. Pozzi, D. Prattichizzo, N. Tsagarakis, and A. Ajoudani, "Grasp stiffness control in robotic hands through coordinated optimization of pose and joint stiffness," *IEEE Robotics and Automation Letters*, vol. 3, no. 4, pp. 3952–3959, October 2018.

[27] Smooth-On. Ecoflex series technical overview. Accessed: 2024-02-29. [Online]. Available: https://www.smooth-on.com/tb/files/ECOFLEX_SERIES_TB.pdf

[28] "The pneumaticbox control system for soft hand control," https://www.tu.berlin/robotics/infrastruktur-und-tutorials/software-tutorials/the-pneumaticbox-control-system-for-soft-hand-control, accessed: 2024-02-29.

[29] G. Salvietti, I. Hussain, M. Malvezzi, and D. Prattichizzo, "Design of the passive joints of underactuated modular soft hands for fingertip trajectory tracking," *IEEE Robotics and Automation Letters*, vol. 2, no. 4, pp. 2008–2015, 2017.

[30] G. Salvietti, Z. Iqbal, I. Hussain, D. Prattichizzo, and M. Malvezzi, "The co-gripper: A wireless cooperative gripper for safe human robot interaction," in *2018 IEEE/RSJ International Conference on Intelligent Robots and Systems (IROS)*, 2018, pp. 4576–4581.

[31] B. Calli, A. Walsman, A. Singh, S. Srinivasa, P. Abbeel, and A. M. Dollar, "Benchmarking in manipulation research: Using the yale-cmu-berkeley object and model set," *Robot. Automat. Mag.*, vol. 22, 2015.

[32] "Tracker, Open Source Physics (OSP)." https://physlets.org/tracker/, accessed: 2024-02-29.

[33] A. Bhatt, A. Sieler, S. Puhlmann, and O. Brock, "Surprisingly robust in-hand manipulation: An empirical study," *arXiv preprint arXiv:2201.11503*, 2022.

[34] D. Prattichizzo, M. Malvezzi, M. Gabiccini, and A. Bicchi, "On motion and force controllability of precision grasps with hands actuated by soft synergies," *IEEE transactions on robotics*, vol. 29, no. 6, pp. 1440–1456, 2013.